

## NUMERICAL MODELING AND EVALUATION OF STEEL FRAMES WITH CONCRETE SLAB

S. Motoyui<sup>1</sup>, K. Kasai<sup>2</sup>, K. Kaneko<sup>3</sup> and T. Asahi<sup>4</sup>

<sup>1</sup> Associate Professor, Dept. of Built Environment, Tokyo Institute of Technology, Yokohama, Japan

<sup>2</sup> Professor, Structural Engineering Research Center, Tokyo Institute of Technology, Japan

<sup>3</sup> Former Postdoctoral research fellow, Center for Urban Earthquake Engineering, T. I. T., Japan

<sup>4</sup> Former Graduate student, Dept. of Built Environment, T. I. T., Japan

Email: [motoyui@enveng.titech.ac.jp](mailto:motoyui@enveng.titech.ac.jp)

### ABSTRACT :

The properties like the rigidity of a frame are very important to predict the dynamic response of the building with any dampers since the effect of dampers in a frame strongly depends on the rigidity of the frame. However, in the case of steel frames to which concrete slabs are attached, the mechanism for the transmission of forces between steel frames and concrete slabs has not been clarified sufficiently and the appropriate numerical model has not established while steel frames without concrete slabs can be accurately simulated recently. The objective in this paper is the establishment of the suitable numerical model to accurately predict the behavior of the damped steel building in the full-size shaking-table test in future. Finally, we examine the validity of the present model in comparison with some experimental results.

**KEYWORDS:** Composite beam, Numerical simulation, Modeling, Material nonlinearity

### 1. INTRODUCTION

The dynamic characteristics in earthquakes of steel buildings with any dampers, depend on the rigidity of steel frames since the effect of dampers in steel frames strongly depends on the rigidity of the steel frames. Therefore, we should grasp the rigidity of a steel frame accurately in the structural design of a damped steel building. In the case of a simple steel structure without concrete slabs and non-structural components, the rigidity of such a structure may accurately be predicted by using the finite element method. On the other hand, a steel building naturally includes concrete slabs and the full-size damped steel building specimen which will be tested in March 2009, also have slabs. In this case, it is difficult to predict the rigidity of such frames accurately because the influence of concrete slabs on the rigidity of steel frames has not been clear. For examples, the number of stud bolts which are used as connection members is usually decided only in order to satisfy the balance of forces between a steel frame and a concrete slab in AIJ Recommendation( AIJ 1985). It is unknown whether the stud bolt group decided so, can keep the section of composite beam being plane (plane-section condition). If it is false, the rigidity can not be found easily using the classical beam theory. Furthermore, it is not obvious what kind of numerical model is suitable to simulate a steel beam with a concrete slab. The main reason is that the mechanism for the transmission of forces between a steel frame and a concrete slab has not been clarified sufficiently, and any numerical modeling for such structures have not been verified. Numerical modeling should involve the essence of a target structure and make it possible to simulate the mechanism faithfully. As a consequence, the load-displacement relation and so on, inevitably agrees with experimental results.

Our objective in this paper is the establishment of an appropriate numerical modeling for steel frames with concrete slabs in order to predict the behavior of the full-sized damped steel building specimen in future. Based on various achievements obtained in the past researches, the useful models for materials and connection conditions are selected and applied to components. In this paper, we use shell elements for steel members of wide flange beams and concrete slabs since we also need to estimate values of local stresses and the locally yielding behavior at the above project. The concept of the present modeling, however, is applicable for numerical analyses using beam elements. Finally we show some numerical examples to verify our modeling. Our numerical results are compared with the past experimental ones. The numerical results are computed with the nonlinear finite element analysis program which has been developed at Motoyui laboratory.

## 2. MODELING FOR MATERIAL

Our main object in this paper is to suggest an appropriate modeling to simulate steel frames with concrete slabs numerically. The appropriate modeling should involve the performance of higher accuracy, better convergence and reduction of CPU time. Therefore, we should extract significant factors from the mechanical characteristics of composite structures and apply simpler models to the extracted factors. In this section, we describe the modeling for material properties after yielding of steel frames and concrete slabs.

### 2.1. Steel

The Baushinger effect of steel has great influence on the post-yielding behavior during cyclic loading. It is also important to consider the residual stress by welding etc. since the residual stress decreases the substantial yield stress. For the consideration of these effect, the Overlay model is applied to the material property model for shell elements by which steel frames are divided. According to the Mises yield criterion,  $J_2$  flow rule and combined hardening rule, stress tensors and tangent coefficient tensor are calculated independently at each virtual layer in the Overlay model. The virtual layer number is set to 14 in this paper. The distribution of the yield stresses on virtual layers are set as shown in Figure 1. The distribution is decided to agree with the past experimental result obtained with the uni-axial cyclic loading test for the standard mild steel in Japan. Figure 2 is the comparison of a numerical result with experimental one. The numerical result is almost close to the experimental one

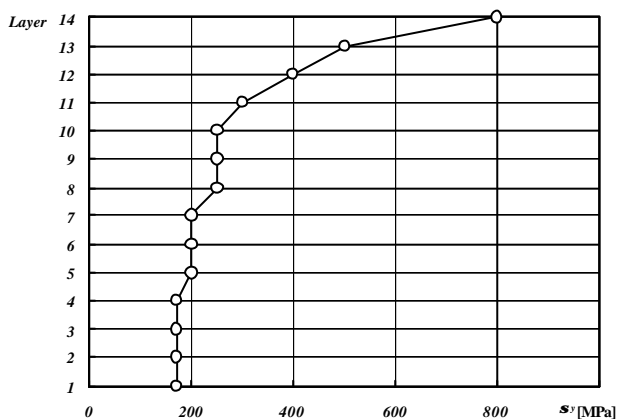


Figure 1 Distribution of Yield Stress on virtual layers

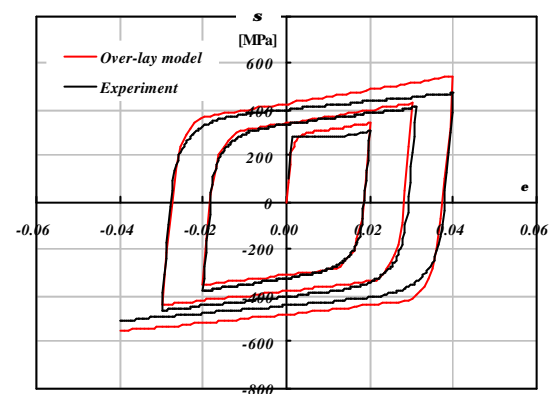


Figure 2  $s$ - $e$  curve ( Uni-axial stress condition)

### 2.2. Concrete

The material models for brittle materials like concrete have been suggested by many researchers. We now select the Barcelona model as the yield function. This function can be expressed as

$$F(s) = \frac{1}{1-a} \left[ aI_1 + \sqrt{3J_2} + bH(t_{\max})t_{\max} \right] - c_c \quad (2.1)$$

where  $I_1$  and  $J_2$  are the first invariant of a stress tensor and the second invariant of a deviatoric stress tensor,  $t_{\max}$  is the maximum principal stress for the plane stress field in shell elements,  $a$  and  $b$  are non-dimensional parameters which should be decided through the material test results,  $H(\cdot)$  is the Heaviside function. This yield function was suggested by Lubliner, Oliver, Oller, Onate 1989 and also used by Lee, Fenves 2001. Their models can evaluate the degradation phenomenon of elastic stiffness after crack of concrete introducing damage parameters. However, for simplicity and convergence at numerical iterative calculations, we do not consider the degradation phenomenon of concrete and any hardening or softening behavior. Generally speaking, our treatment in which the degradation is ignored is not appropriate. However, if the effect of concrete slabs on steel frames can not be neglected but can be assumed to be only secondary, the treatment is the reasonable approximation. The elastic region defined with Eqn.2.1 in the principal stresses space is shown in Figure 3. Here,  $a$  is set to 0.12 and 0.08.

The non-associative flow rule is assumed for the plastic flow rule as followings

$$\dot{\epsilon}_p = \frac{\partial F}{\partial \mathbf{s}} \dot{\mathbf{g}} = \left( \frac{\tilde{\mathbf{s}}}{\|\tilde{\mathbf{s}}\|} + \hat{\mathbf{s}} \mathbf{I} \right) \dot{\mathbf{g}}, \quad F(\bar{\mathbf{s}}) = a_p I_1 + \sqrt{J_2} \quad (2.2)$$

where  $\dot{\epsilon}_p$  is a plastic strain rate tensor,  $\tilde{\mathbf{s}}$  and  $\hat{\mathbf{s}}$  are a deviatoric stress tensor and a mean stress,  $\mathbf{g}$  is a consistent plastic parameter and  $F$  is a potential function which is defined as Eqn.(2.2b). By applying the non-associative flow rule, the tangent coefficient tensor after yielding becomes to be non-symmetric. As a result, the global tangent stiffness matrix falls into an un-symmetric matrix.

$$d\bar{\mathbf{S}} = \left\{ \mathbf{E}'' - \frac{1}{H_{total}} \mathbf{E}'' \left( a_p \mathbf{I} + \frac{\tilde{\mathbf{s}}}{\|\tilde{\mathbf{s}}\|} \right) \otimes \mathbf{E}'' \left( a \mathbf{I} + \sqrt{\frac{3}{2}} \frac{\tilde{\mathbf{s}}}{\|\tilde{\mathbf{s}}\|} + \bar{b} \frac{\partial t_{max}}{\partial \mathbf{s}} \right) \right\} d^v \mathbf{e} \quad (2.3)$$

$$H_{total} = \left( a \mathbf{I} + \sqrt{\frac{3}{2}} \frac{\tilde{\mathbf{s}}}{\|\tilde{\mathbf{s}}\|} + \bar{b} \frac{\partial t_{max}}{\partial \mathbf{s}} \right) : \mathbf{E}' \left( a_p \mathbf{I} + \frac{\tilde{\mathbf{s}}}{\|\tilde{\mathbf{s}}\|} \right) \quad (2.4)$$

$$\mathbf{E}'' = \left( \frac{1+n}{E} + \frac{D\mathbf{g}}{\|\tilde{\mathbf{s}}\|} \right)^{-1} \left[ \mathbf{I}_4 + \left( \frac{n}{1-2n} + \frac{1}{3} \frac{E}{1-2n} \frac{D\mathbf{g}}{\|\tilde{\mathbf{s}}\|} \right) (\mathbf{I} \otimes \mathbf{I}) + \frac{E}{1+n} \frac{D\mathbf{g}}{\|\tilde{\mathbf{s}}\|} \frac{\tilde{\mathbf{s}}}{\|\tilde{\mathbf{s}}\|} \otimes \frac{\tilde{\mathbf{s}}}{\|\tilde{\mathbf{s}}\|} \right] \quad (2.5)$$

We do not artificially symmetrize the stiffness matrix but directly solve simultaneous equations with un-symmetric coefficient in order to prevent the iterative calculation from being the bad convergence condition.

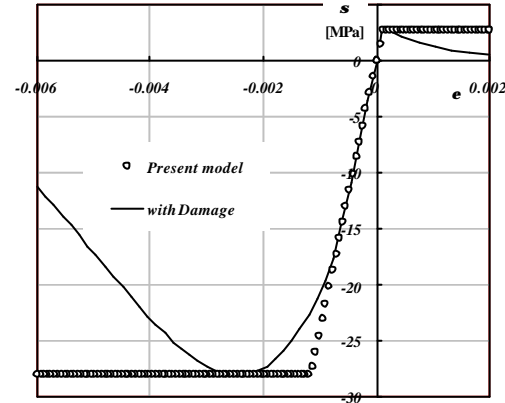
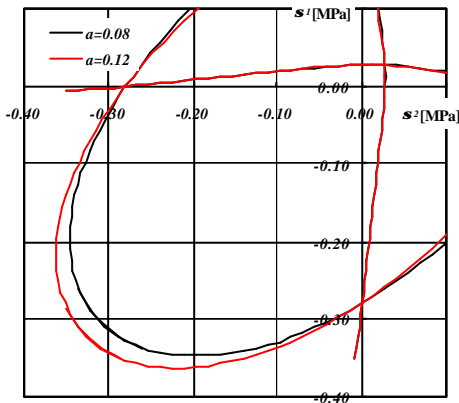


Figure 3 Yield function in principal stresses space      Figure 4  $s$ - $e$  curve ( Uni-Axial stress condition)

### 3. MODELING OF INTERACTION BETWEEN STEEL FRAME AND CONCRETE SLAB

#### 3.1 Hysteresis curve for Stud Bolt

Concrete slabs are connected to steel frames using stud bolts. The necessary number of stud bolts ( $n_r$ ) between the point where the plastic hinge occur and the inflection point, are calculated through the horizontal shear force estimated as (AIJ 1985)

$$n_r = \frac{Q_h}{q_s}, \quad Q_h = \min(0.85 A_c F_c, A_s s_y), \quad q_s = 0.5 a_s \sqrt{F_c E_c} \quad (3.1)$$

where  $Q_h$  and  $q_s$  are the design horizontal shear force and the shear strength of a stud bolt,  $A_s$ ,  $s_y$  are a cross section area of a steel beam,  $F_c$  and  $E_c$  are a compressive strength and Young's modulus of concrete and  $a_s$  is a section area of a stud bolt,  $A_c$  is defined with the product of a effective width which is calculated by  $0.1 \times (\text{Length of a span})$  and thickness of a concrete slab. It is noted that only the balance of force at the ultimate state is

considered by using Eqn(3.1). The stud bolt number found by Eqn(3.1) does not always satisfy the plane-section assumption. Generally the rigidity only with the stud bolt number is much less than the necessary rigidity for stud bolts to hold the plane-section condition. The matter means that the value of the bending rigidity for a steel beam with a concrete slab is less than calculated one based on the elastic beam theory with plane-section condition. Therefore, the modeling for the connection by stud bolts should be set carefully.

We set such a shear force and gap between concrete and steel member relation for the monotonic loading as agrees with the result of the experiment by Inoue, et.al. 1988. Furthermore, the hysteresis model for stud bolts in shear was suggested by Yamanobe et.al. 1997. According to the model, the hysteresis for stud bolts in cyclic loading is the slip type. Then we apply the solid line in Figure 6 to the shear force and gap relation. It is noted that the results of the experiment as shown in Figure 5 include the interaction between stud bolts and concrete, and our hysteresis model for the connection with stud bolts reflects the effect of the damage of concrete near stud bolts.

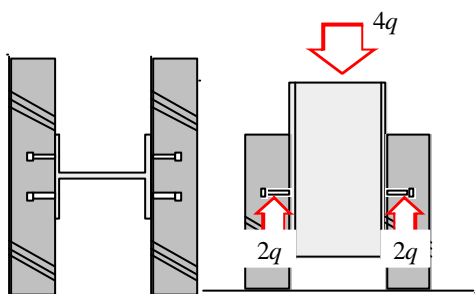


Figure 5 Standard test for stud bolts

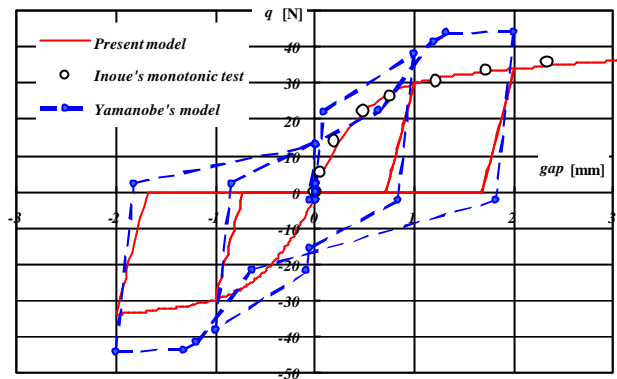


Figure 6 Shear force – gap between concrete and steel member relation

### 3.2 Setup of parts

In this paper, steel frames and concrete slabs are divided with 4-node shell elements(Dvorkin and Bathe 1984), and for each stud bolt a 2-node co-rotational beam element(Crisfield 2000) is used. Shell elements mapped on the mid surface of a concrete slab are connected to shell elements on the mid-surface of flange plate at steel beams using beam elements of stud bolts as shown in Figure 7(a). Figure 7(a) is the diagram for the concrete slab with steel decks. In such concrete slabs, we assume that the shadow area shown in the figure is only active , and slabs are plates with uniform thickness( $t'$ ) though the slab thickness is not uniform actually.

On the other hand, it was pointed out that the transmittance of a force via a contact surface of a concrete slab with a steel column had the great influence on the concrete slab-steel frame interaction mechanism (Inoue et.al. 1999). For the transmission of force, we set three group of dummy beam elements as shown in Figure 7(b).

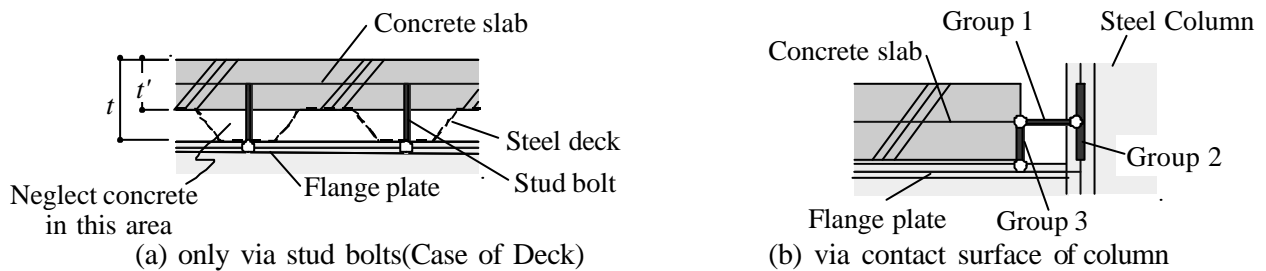


Figure 7 Connection model

Group 1 represents the contact behavior between concrete slabs and steel column. This group become to be inactive during tensile forces act on themselves like so-called gap element. Group 2 is set to avoid the extreme stress concentration at the point where Group 1 is connected. Group 3 is to prevent from concrete slabs' penetration into flange plates. The beam elements in Group 1-3 are assumed to be rigid and ones in Group 2 have only the bending rigidity and their axial rigidity is set to zero not to disturb axial stress condition in steel columns.

## 4. NUMEIRCAL EXAMPLES

### 4.1 Outline of Specimen

Here, we verify our modeling through the comparison of numerical results and experimental ones and consider the influence of the different type of modeling on the numerical results. An example is only single wide flange steel beam with a concrete slab tested by Inoue, Igarashi et.al. 1984. In this experiment, rigid steel end-plates are set at both end of a beam to represents steel columns. The geometry and dimension in this test are shown in Figure 8. The mechanical properties of steel plate, concrete and stud bolt is shown in Table 1.

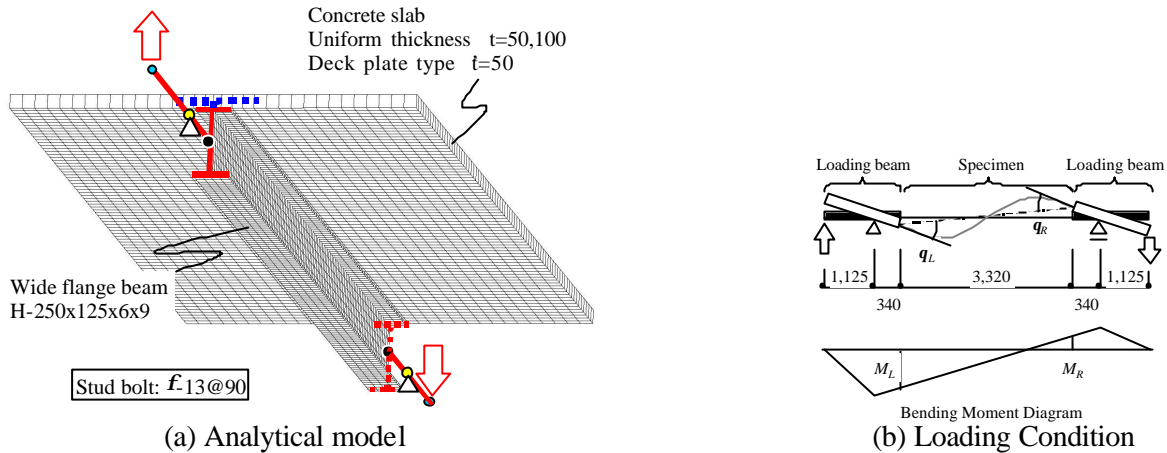


Figure 8 Numerical examples [ unit : mm ]

Table 4.1 Mechanical properties

Web PL-6	$s_y=334\text{MPa}$
Flange PL-9	$s_y=295\text{MPa}$
Stud Bolt	$q_s=36.2\text{kN}$
Concrete	$F_c=28.0\text{MPa}$

### 4.2 Numerical results and consideration

At first, the result for only steel test specimen in cyclic loading is shown in Figure 9. This figure is the relation between  $M_R+M_L$  and  $q$  ( See Figure 8(b) ). Thick line is the experimental result and another is numerical one. To understand clearly, we compare these results by 2 cycles.

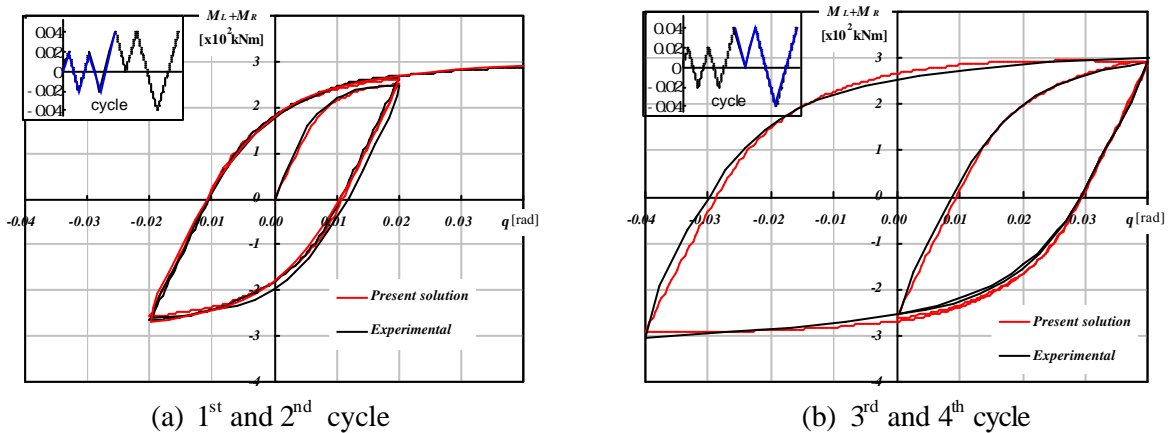


Figure 9 Comparison between Numerical and Experimental results – Steel –

In both the smaller and the larger deformation level, the present solution is very close to the experimental result. Especially the present material model for steel does not have the yield plateau. Nevertheless, the good

agreement is also observed at initially yielding state. The matter means that the substantial yield stress decreases in the existence of the residual stress and the stress-strain relation falls into the round-house type.

Next, compare the results for specimen with concrete slabs. It is expected that the condition of a concrete slab has the influence on the rigidity, strength and stress condition of a steel frame. It is important whether the behavior of composite beams with various type of slabs can be simulate by the present model, because it is our objective to predict the behavior of the full-sized damped steel building specimen accurately.

Figure 10 shows the results for concrete slabs with two types of thickness ( (a) $t=100\text{mm}$ , (b) $50\text{mm}$ ). The initial rigidity and post-yielding behavior with the present solutions generally agree with ones by the experimental results though slight difference after yielding is observed in the case of  $t=50\text{mm}$ .

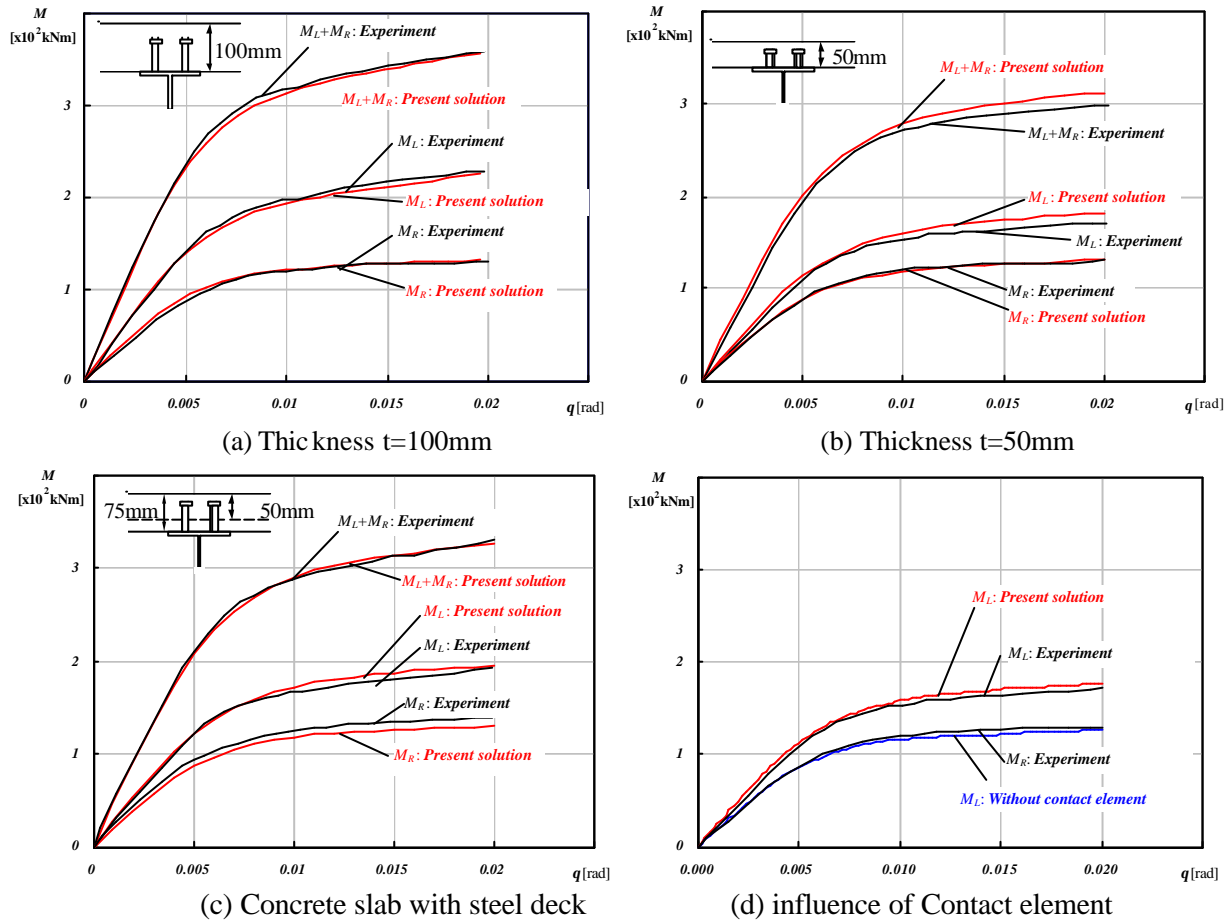


Figure 10 Comparison between Numerical and Experimental results – Composite –

The above two examples are composite beams with uniform concrete slabs. We show the performance of the present model for non-uniform concrete slabs with steel decks in Figure 10(c). It is understood that the present model is effective to such a composite beam.

We emphasized that the transmission of forces via the contact surface between a concrete slab and a steel column has the great influence on the behavior of a composite beam. To evaluate the effect of the contact, compare results with the model in which all dummy groups (contact elements) in Figure 8 are eliminated with the present solution. Figure 10(d) shows  $M_L$ - $q$  relationship. The result by the model without contact elements is fairly different from experimental ones and becomes to be close to  $M_R$  by experiment. Figure 11 shows the distribution of the equivalent stress. The equivalent stress of the concrete slab near the column in the model with contact elements, became greater than one in the model without contact elements. As a result, the equivalent stress distribution in steel beams becomes different from each other (Figure 11(a)). In the model without contact elements, the neutral axis keeps the position at the mid-axis of a beam similar to an only steel beam model while the neutral axis moves to the upper direction in the model with contact elements. Therefore, the contact elements presented in this paper are necessary to simulate the behavior of composite beams accurately.

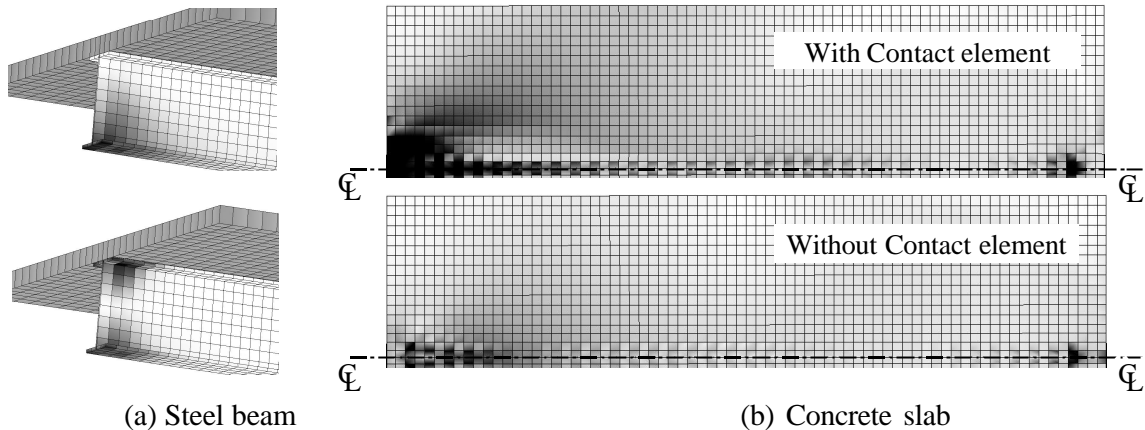


Figure 11 Distribution of equivalent stress (Upper: Taking account of contact elements, Lower: none)

Finally, we show the results for composite beams ( $t=100\text{mm}$ ) under cyclic loading. Figures 12(a)-(c) are the relation between  $M_R+M_L$  and  $q$ . The result at each cycle is shown sequentially. Generally the results by the present model are close to the experimental ones. Particularly the rigidity and post-yielding behavior obtained by the present model agree with ones by the experiment in the smaller deformation level ( See Figure 12(a)-(b) ). However, the results have discontinuous points that are shown by  $\Delta$  in the figures on the equilibrium path. The discontinuous points occur at the time of re-contact of the concrete slab to the column after separating them.

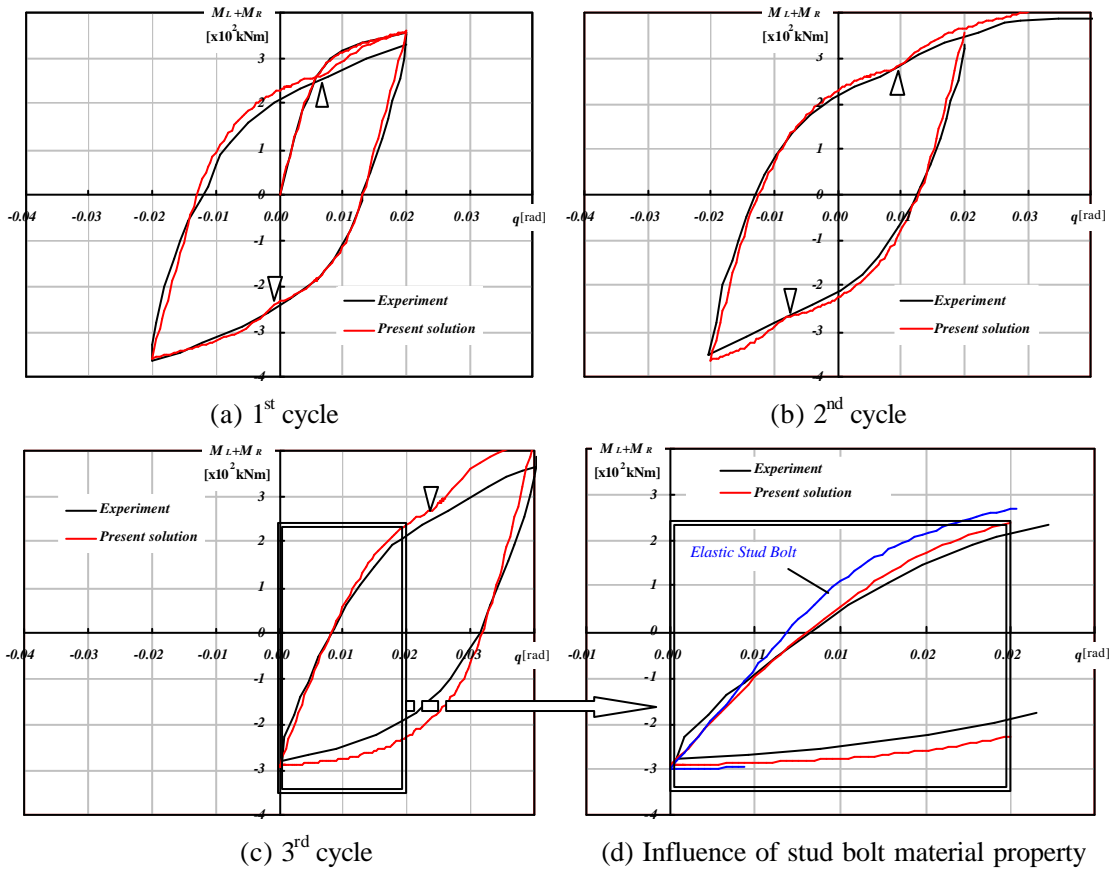


Figure 12 Comparison between Numerical and Experimental results – Composite under cyclic loading –

The discontinuous phenomenon is also observed in the experimental results but is not as remarkable as the present ones. The reason is that concrete near the contact surface is damaged and the in-plane rigidity of a

concrete slab is degraded. We assumed that contact elements is rigid in this paper, but should consider the more suitable mechanical properties for them to simulate the collapse behavior of composite beams under cyclic loading like an earthquake. On the other hand, the slight difference for the stiffness between both results, is observed at the start of unloading. The stiffness obtained by the experiment has reduced to one for the only steel specimen (Refer to Figure 9). It can be expected that the reduction is caused by the damage of concrete, especially concrete near stud bolts. The reduction depends on the mechanical characteristics of connection of a concrete slab to steel beams. For the sake of simulating such phenomenon, we introduced the especial hysteresis curve for stud bolts. To confirm the effect of the hysteresis curve of stud bolts, the present results are compared with the results by the model with elastic stud bolts in Figure 12(d). From this figure, it can be understood that the result of the present model represents the damage at the connection between concrete slabs and steel beams better than one of the elastic stud bolt. Therefore, more suitable mechanical model for the connection with stud bolts should be considered in future.

## **5. CONCLUSION**

We have suggested the numerical modeling for steel beams with concrete slabs and verified the modeling through some numerical examples. By using our proposal modeling, the behavior of composite beams can be simulated and the rigidity and post-yielding behavior can be predicted highly accurately. We expect that the performance of our modeling is enough to predict the response of the damped steel building specimen which is sensitive to the rigidity etc. of a frame. Unfortunately the gap between numerical results and experimental ones was observed in the larger deformation level where concrete was damaged remarkably. To overcome such problem, we shall improve the mechanical characteristics of contact elements and stud bolts which involve the local damage of concrete in future.

## **ACKNOWLEDGEMENTS**

This study is a part of “NEES/E-Defense collaborative research program on steel structures”, and was pursued by the Analysis Method and Verification WG. The Japan team leader for the overall program Kazuhiko. Kasai at Tokyo Institute of Technology and the WG leader is Motohiko Tada at Osaka University. The writers acknowledge the support of members of Damper Isolation System WG (leader: Kazuhiko Kasai) and financial support provided by the National Research Institute for Earth Science and Disaster Prevention.

## **REFERENCES**

- Architectural Institute of Japan. (1985). Design Recommendations for Composite Construction 1985 (in Japanese)
- Crisfield, M.A. (2000). Nonlinear Finite Element Analysis of Solids and Structures, Vol.2, John Willey & Sons
- Dvorkin, E.N. and Bathe, K.J. (1984). A continuum mechanics based four-node shell element for general nonlinear analysis, Engineering Computations Vol.1, 77-85
- Inoue, K., Kim, S. and Igarashi, S. (1984). Experimental study on stiffness and strength of composite beams, Transactions of the Architectural Institute of Japan, No.344, 68-80 (in Japanese)
- Inoue, K., Tsujioka, S. and Arai, T. (1988). Positive Bending Strength of Composite Beams at Beam-to-Column Connection : Part 1. Bearing and Shear Strength of Reinforced Concrete Slabs, Summaries of technical papers of Annual Meeting Architectural Institute of Japan. Structures II, 1157-1158 (in Japanese)
- Lee, J. and Fenves, G.L. (2001). A return mapping algorithm for plastic-damage models : 3-D and plane stress formulation, International Journal of Numerical Method in Engineering, 50, 487-506
- Lubliner, J., Oliver, J., Oller, S. and Onate, E. (1989). A plastic -damage model for concrete, International Journal of Solids and Structures, Vol.25, No.3, 299-326
- Yamanobe, K., Yabe, Y. and Wada, A. (1997). 2dimensional elasto-plastic analysis of steel frames with composite beams incorporating structural non-linearity of headed studs, Journal of structural and construction engineering. Transactions of AIJ, No.502, 135-140 (in Japanese)